Correlation of bonding of grain boundary and fracture mode with local electronic structure in steels by electron energy loss spectroscopy

X. Zhang,[a] W. G. Yang, L. N. Zhang, J. J. Qi, and J. Yuan
Laboratory of Advanced Materials, Department of Materials Science and Engineering, Tsinghua University, Beijing 100084, People's Republic of China and National Center for Electron Microscopy (Beijing), Beijing 100084, China

(Received 2 February 2007; accepted 28 March 2007; published online 23 April 2007)

Electron energy loss spectroscopy (EELS) was used to study bonding of grain boundaries (GBs) in various types of commercial steels. It is found that if the GB has a higher occupancy of 3*d* states of iron than that of the grain, the sample tends to fracture intergranularly. Otherwise if the GB has a lower occupancy of 3*d* state of iron than the grain, the sample would have a strong GB bonding and tends to fracture transgranularly. It is proposed that EELS can estimate the GB cohesion and its impact on the fracture mode of commercial steels. © *2007 American Institute of Physics*. American Institute of Physics [DOI: 10.1063/1.2731687]

It is generally accepted that grain boundary (GB) embrittlement phenomenon in steels is associated with the segregation of the impurities belonging to groups 4A to 6A of the Periodic Table, and the impurity segregation leads to a reduction in the cohesion of grain boundaries.[1–4] As a result the mechanical properties of the materials change significantly.

High-resolution transmission electron microscopy and energy dispersive spectroscopy (EDS) are common tools to study the grain boundaries. However, these techniques cannot directly provide the information about the bonding of atoms at GB. To study the cohesion of GB, people normally use Charpy V-notch impact test and examine the fracture surface of the sample using scanning electron microscopy. If the sample fractures intergranularly, the cohesion of the GB is said to be weaker than that of the grain; whereas if the sample fractures transgranularly, the GB may not be the weak link. But Charpy V-notch impact test is a macroscopic method and one cannot choose a specific GB to perform the impact test. Also this method cannot relate the impurity segregation to the bonding of the GB. However, it is important to know if some element segregations at GB will weaken or enhance the bonding of GB. Therefore it is a challenge to develop a microscopic method being capable to choose a specific GB for studying the bonding of the GB and relating the impurity segregation with the bonding of the GB.

As bonding of GB is related to the local electronic structure at GB, electron energy loss spectroscopy (EELS) may play a useful role here. For transition metals, their L_2 and L_3 absorption edges in the EELS spectra show very sharp peaks called "white lines."[5–7] Pearson *et al.*[7,8] studied 3*d* and 4*d* transition metals and found that changes in normalized intensities of the white lines could be used to measure changes in the occupancies of the associated *d* states of transition metals. Muller *et al.*[9,10] studied boron doping effect in Ni_3Al. They measured the white line intensities of Ni EELS and correlated them with the fracture mode and environmental embrittlement of the alloy. Similarly, Özkaya *et al.*[11,12] have studied the phosphor doped high purity iron and have found that the 3*d* state is also related to the level of P segregation. As P is known as an embrittler, then the question naturally arises if the 3*d* occupancy itself can be a reliable guide of coherence of the grain boundary in ordinary steel where alloy chemistry is much more complex. For the same reason of the complexity of the alloy steel systems, the theoretical calculation is still not realistic enough to give a definite answer.

In this work, we study directly the correlation of 3*d* occupancy of Fe in a number of different steels with their fracture behavior by using transmission electron microscopy (TEM), scanning transmission electron microscopy (STEM), EELS, and EDS techniques. We will show that the 3*d* occupancy change is a good indicator of the grain boundary bonding change. Our result also shows the influence of different impurities present.

Four commercial steels and pure iron were used in this work and their chemical compositions are listed in Table I. Samples 1 and 2 are commercial 42CrMo alloy steels. They were oil quenched at 880 °C for 15 min and then aged at 350 and 550 °C for 120 min, respectively. Sample 3 is a CrMo steels (ADF1). It was oil quenched at 850 °C for 30 min and then tempered at 585 °C for 120 min. Samples 4 and 5 are No. 45 plain steels. They were oil quenched at 860 °C for 20 min and then aged at 350 and 600 °C, respectively, for 120 min. Samples 6 and 7 are commercial 40Cr alloy steels. They were water quenched at 860 °C for 20 min and then aged at 350 and 600 °C, respectively, for 120 min. Pure iron (99.95%, weight percent is used in this letter) was also used in this work.

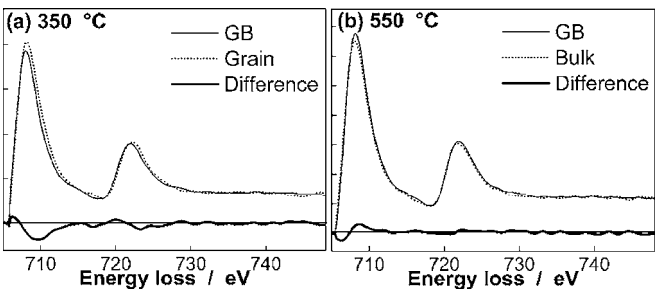

FIG. 1. EELS spectra of Fe $L_{2,3}$ absorption edge of a 42CrMo steels measured at the grain boundary (GB), in the grain and their difference in (a) sample 1 and (b) sample 2.

[a]Electronic mail: xzzhang@tsinghua.edu.cn

TABLE I. Chemical compositions of the experimental steels (wt %).

Metal	C	Si	Mn	Cr	Mo	P	S
42CrMo	0.39	0.29	0.80	1.08	0.22	0.025	0.019
ADF1	0.43	0.14	0.30	1.10	0.52	0.003	0.001
No. 45	0.45	0.27	0.60	0.02	0.00	0.061	0.003
40Cr	0.40	0.33	0.62	1.03	0.02	0.071	0.003
Pure iron	0.028	0.17	0.031	···	···	0.014	<0.0015

In this work, EELS and EDS were performed using a field emission gun TEM (JEM-2010F) equipped with EDS (Link ISIS) and EELS (GIF 678, Gatan). The microscope was operated in the STEM mode with a spot size of 0.5 nm in diameter at 200 kV. The GB plane was oriented parallel to the beam direction. The electron beam was allowed to pass through the specimen on and off the GB, so that the composition and EELS of the GB and grains can be analyzed. When acquiring EELS, the spectrometer collection aperture used is 2 mm in diameter and the energy dispersion is set at 0.2 eV/channel. All spectra are background subtracted using the power law function and then deconvoluted by the Fourier-ratio method to remove multiple scattering components. We measured the normalized intensities of the Fe white lines in the EELS spectra and calculated the occupancies of the $3d$ state using the method by Pearson *et al.*[7] The details of the experiments can be found in Ref. 13.

Under the Charpy V-notch impact test performed at room temperature, samples 1, 4, and 6 fracture intergranularly, whereas samples 2, 3, 5, and 7 fracture transgranularly (Table II). Sample 8 is a pure iron that fractures transgranularly.

EELS spectra of Fe L edges of the samples 1 and 2 were collected at GB and at grains, respectively (Fig. 1). For sample 1, the intensity of the $L_{2,3}$ peak decreases in the spectrum of the GB compared with that of the spectrum of the grain. However, the result is opposite in sample 2. In order to correlate the spectra features with the electronic structure of Fe, we measured the normalized intensities of iron white lines in the EELS spectra and calculated the occupancies of the $3d$ states (n_{3d}) of iron following the method by Pearson *et al.*[7]

In our experiments, the size of the probe used for measuring EELS is measured and it is about 0.7 nm in diameter. The width of its projection corresponds to about three atomic layer spacing in steels. For simplicity, the probe is thought to be smaller than the width of the GB region, and we suppose the change in the Fe d electron occupancy around the GB region distributes as step functions, as shown in Fig. 2. Our analysis shows that the n_{3d} at the GB is larger than that in the grain in sample 1. The Δn_{3d}, the outcome of subtracting the n_{3d} at the GB from that in the grain, has a positive value of 0.49 e/at., whereas the Δn_{3d} in sample 2 has a negative value of −0.16 e/at.. As sample 1 fractures intergranularly and sample 2 fractures transgranularly (Table II), we conclude that if the GB has a higher occupancy of $3d$ states than the grain (corresponding to the positive Δn_{3d}), the sample tends to fracture intergranularly; whereas if the GB has a lower occupancy of $3d$ states than the grain (corresponding to the negative Δn_{3d}), the sample tends to fracture transgranularly. This conclusion is shown schematically in Fig. 2.

The temper embrittlement phenomenon of sample 1 is probably attributed to the impurity segregation at the GB when aged at the temperature of 350 °C.[1–3] In commercial steels, the impurity elements mainly refer to P and S. The EDS analysis was performed to measure the element segregation to GB, and the results are shown in Table II. It is found that all the samples with intergranular fracture (samples 1, 4, and 6) have a little P segregation at GB, and they all have positive values of Δn_{3d}. Whereas all the samples with transgranular fracture (samples 2, 5, and 7) have no P segregation at GB, they all have negative values of Δn_{3d}. It appears that P segregation at GB does play an important role on intergranular fracture.

TABLE II. EDS results of element segregation at GB of various steels (wt %). TA, FM, I, and T represent age temperature, fracture mode, intergranular, and transgranular, respectively.

	Metal	TA (°C)		P	S	Mo	Δn_{3d}	FM
			GB	0.09±0.08	0.08±0.19	0.1±0.5		
1		350	Grain	0.01±0.03	0.03±0.09	0.3±0.5	0.49±0.06	I
			GB	0.03±0.06	0.04±0.15	0.4±0.6		
2	42CrMo	550	Grain	0.04±0.08	0.04±0.11	0.1±0.3	−0.16±0.05	T
			GB	0.00±0.01	0.00±0.01	1.2±0.3		
3	ADF1	585	Grain	0.00±0.01	0.00±0.01	0.5±0.1	−0.24±0.08	T
			GB	0.08±0.07	···	···		
4		350	Grain	0.07±0.10	···	···	0.29±0.06	I
			GB	0.05±0.06	···	···		
5	No. 45	600	Grain	0.05±0.06	···	···	−0.38±0.06	T
			GB	0.11±0.10	···	···		
6		350	Grain	0.09±0.13	···	···	0.57±0.08	I
			GB	0.07±0.08	···	···		
7	40Cr	600	Grain	0.07±0.10	···	···	−0.23±0.07	T

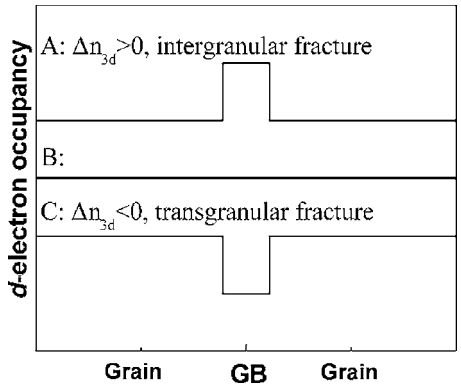

FIG. 2. Three distributions of Fe *d*-electron occupancy around GB region. Curves A, B, and C represent Fe *d*-electron occupancy at GB is larger, equal, and smaller than that in grain, respectively.

Mo was generally considered as a cohesion enhancer at GB in steels.[3,14–18] Our technique for studying bonding of GB using EELS provides a way to test the above result. We used EELS to measure bonding of the GB in sample 3 of a CrMo steels (ADF1) developed based on 42CrMo steels, which has a similar chemical composition as samples 1 and 2 but a higher Mo content of 0.5%. EDS analysis of a GB in sample 3 (not shown) reveals that Mo segregates significantly at the GB. EELS experiments show that the occupancy of 3*d* states is smaller (Δn_{3d} is −0.24 *e*/at.) at the GB than in the grain. According to the conclusion we have drawn above, sample 3 may fracture transgranularly, and this is verified by the impact test (Table II).

Because there are alloy elements other than P or Mo in samples 1 and 3, it is difficult to exclude their contribution to Δn_{3d}. In order to identify the effect of P and Mo in steels on the Δn_{3d}, we prepared pure iron, Fe–P0.01% and Fe–P0.012%–Mo2.1% alloys. The Fe–P0.01% and Fe–P0.012%–Mo2.1% samples were homogenized at 1000 °C for 1 h, cooled by air to room temperature, then aged at 350 °C for 50 h for P and Mo to segregate. The EELS results of the samples are shown in Table III. The pure iron has a negative Δn_{3d} of −0.41, indicating that the sample fractures transgranularly as expected. The Fe–P0.01% alloy has a positive Δn_{3d} of 0.54, indicating that the sample fractures intergranularly. When Mo is added into the alloy, Δn_{3d} of Fe–P0.012%–Mo2.1% alloy decreases to a negative value of −0.12. Considering that the Δn_{3d} of pure iron is −0.41, one can see clearly that P segregation at GB leads to increase of Δn_{3d}, and Mo segregation at GB can suppress the increase of Δn_{3d} induced by P. This may be the mechanism that P segregation at GB leads to temper embrittlement, whereas Mo often acts as cohesion enhancer.

TABLE III. Effect of P and Mo on Δn_{3d} of iron.

	P (wt %)	Mo (wt %)	Δn_{3d}
Pure iron	0.014	···	−0.41±0.06
Fe–P0.10%	0.10	···	0.54±0.08
Fe–P0.12%–Mo2.1%	0.12	2.1	−0.12±0.08

The influence of the microstructure of the GB on Δn_{3d} is also considered. EELSs of three kinds of GBs with different grain orientations were acquired and the occupancies of 3*d* states of pure iron and sample 1 were measured. The results show that the occupancy of the 3*d* states is not significantly influenced by grain orientation, so the contribution of impurity segregation dominated the value of Δn_{3d}.

To test if our proposed EELS method for studying bonding at GB is applicable to other types of steels, EELS spectra of Fe $L_{2,3}$ edge of a 40Cr alloy steel and a No. 45 steel were measured and the Δn_{3d} were calculated correspondingly (Table II). The correlation between the Δn_{3d} and the fracture mode was found to be the same as that of the 42CrMo alloy steels; i.e., if the sample fractures transgranularly, the Δn_{3d} is negative, and if the sample fractures intergranularly, the Δn_{3d} is positive.

In conclusion, EELS spectra of the Fe $L_{2,3}$ edge were used for studying bonding of GB of various types of steel. The Δn_{3d}, the difference between the n_{3d} at GB and in grain, was calculated. It is found that if the value of Δn_{3d} is positive, the GB would have a weak cohesion and the sample tends to fracture intergranularly. Whereas if the value of Δn_{3d} is negative, the GB would have a strong cohesion and the sample tends to fracture transgranularly. The change in n_{3d} is mainly attributed to the impurity segregation at GB. According to the variation of n_{3d} from EELS spectra, we can estimate the cohesion of a GB and detect the impact on the fracture mode of the steels.

The authors would like to thank the financial support by Ministry of Science and Technology (Grant Nos. G1998061514 and 2002CB813501) and National Science Foundation of China (Grant No. 90401013).

[1]C. J. McMahon and V. Vitek, Acta Metall. **27**, 507 (1979).
[2]M. L. Jokl, Jun Kameda, C. J. McMahon, and V. Vitek, Met. Sci. **14**, 375 (1980).
[3]D. Y. Lee, E. V. Barrera, J. P. Stark, and H. L. Marcus, Metall. Trans. A **15A**, 1415 (1984).
[4]M. L. Jokl, V. Vitek, and C. J. McMahon, Acta Metall. **28**, 1479 (1980).
[5]R. F. Egerton, *Electron Energy-Loss Spectroscopy in the Electron Microscope*, 2nd ed. (Plenum, New York, 1996), Chap. 5, 371.
[6]D. A. Muller, Y. Tzou, R. Raj, and J. Silcox, Nature (London) **66**, 725 (1993).
[7]D. H. Pearson, C. C. Ahn, and B. Fultz, Phys. Rev. B **47**, 8471 (1993).
[8]D. H. Pearson, C. C. Ahn, and B. Fultz, Phys. Rev. B **50**, 12969 (1994).
[9]D. A. Muller, S. Subramanian, P. E. Batson, S. L. Sass, and J. Silcox, Phys. Rev. Lett. **75**, 4744 (1995).
[10]D. A. Muller, S. Subramanian, P. E. Batson, J. Silcox, and S. L. Sass, Acta Mater. **44**, 1637 (1996).
[11]D. Özkaya, J. Yuan, L. M. Brown, and P. E. J. Flwitt, J. Mater. Sci. Lett. **180**, 300 (1995).
[12]D. Özkaya, J. Yuan, and L. M. Brown, Inst. Phys. Conf. Ser. **147**, 345 (1995).
[13]X. Z. Zhang, Y. Ma, J. Yuan, M. Q. Wang, L. M. Brown, and L. N. Zhang, ISIJ Int. **l43**, 671 (2003).
[14]B. C. Woodfine, J. Iron Steel Inst., London **173**, 229 (1953).
[15]D. V. Doane, J. Met. **36**, 83 (1984).
[16]S. Suzuki, S. Tanii, K. Abiko, and H. Kimura, Metall. Trans. A **18A**, 1109 (1987).
[17]M. Menyhard and C. J. McMahon, Acta Metall. **37**, 2287 (1989).
[18]W. T. Geng and A. J. Freeman, Phys. Rev. B **62**, 6208 (2000).